Synsint Research Group

Available online at www.synsint.com

Synthesis and Sintering

ISSN 2564-0186 (Print), **ISSN** 2564-0194 (Online)

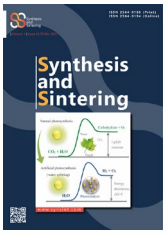

Research article

Sintering behavior and microwave dielectric properties of $CaTi_{1-x}(Nb_{1/2}Al_{1/2})_xO_3$

Akbar Khan*, Asif Ali, Izaz Khan

Laboratory of Functional Materials and Devices, Department of Physics, Abdul Wali Khan University Mardan, 23200 KP, Pakistan

A B S T R A C T

$CaTi_{1-x}(Nb_{1/2}Al_{1/2})_xO_3$ with x=0.1–0.5 ceramics were processed through solid state sintering. X-rays diffraction (XRD) patterns of the compositions showed that the samples have orthorhombic crystal structure with symmetry (Pbnm). The symmetry was further confirmed using Raman spectroscopy. A total of 13 Raman modes were detected, which were in agreement with the XRD results. Microstructure analysis of the samples showed porosity in the samples, presumably due to the substitution of Al, having high melting point. As the concentration of Al and Nb increased, relative permittivity (ε_r), quality factor ($Q\times f_o$) and temperature coefficient of resonance frequency decreased. Optimum microwave dielectric properties were achieved for the composition x=0.5 sintered at 1650 °C for 8 h i.e., ε_r ~27.09, $Q\times f_o$ ~17378 GHz, and τ_f ~ -2.5 ppm/°C.

KEYWORDS

Perovskite
$CaTiO_3$
Microwave dielectric properties

OPEN ACCESS

1. Introduction

Dielectric ceramics are widely used in different communication systems such as cellular phones, satellites, base stations, military radar, navigation system, ITS, automation, filters, oscillators etc. For microwave (MW) applications, appropriate relative permittivity (ε_r), low tan δ or high $Q\times f_o$ and near zero temperature coefficient of resonance frequency (τ_f) are preferred [1–3]. For MW applications, perovskites are of special interest due to their interesting physical and chemical properties. Perovskite structure $CaTiO_3$ was discovered by German mineralogist, Gustav Rose (in 1839) who he named as perovskite in the recognition of a Russian mineralogist L.A. Perovski.

$CaTiO_3$ has orthorhombic structure and exhibit high ε_r = 162, reasonable $Q\times f_o$ (~8354 GHz) but its high τ_f (+803.7 ppm/°C) renders its use in practical applications [4]. To tune τ_f of $CaTiO_3$, A- and/or B-site or both sites have been modified. Tao et al. [5] investigated $[Ca_{1-x}(Li_{1/2}Nd_{1/2})]TiO_3$, while substituting Ca^{2+} by $(Li_{1/2}Nd_{1/2})^{2+}$ at the B-site and obtained optimal MW dielectric properties; ε_r = 112.6, $Q\times f_o$ = 4480 GHz and τ_f = +8.2 ppm/°C at x = 0. $(1-x)CaTiO_3$-$xCa(Ta_{1/2}Ga_{1/2})O_3$ possess ε_r =47, $Q\times f_o$ =26,630 GHz and τ_f ~-2.64 ppm/°C for the x = 0.5 [6]. The effect of La substitution for Ca in $CaTiO_3$ with general formula $Ca_{1-x}La_{2x/3}O_3$ was exhibited $Q\times f_o$ = 17600 GHz, ε_r = 109, τ_f = +213 ppm/°C at x = 0.4 [7]. $Ca_{0.66}La_{0.387}Ti_{0.88}O_3$ possess high $Q\times f_o$ = 13407 GHz and ε_r = 71.5 but a poor τ_f = +136.4 ppm/°C [8]. Feteira et al. [9] observed a decrease in ε_r from 170 to 12, while an increase in $Q\times f_o$ from 10000 to 12000 GHz in compositions $Ca_{1-x}Y_xTi_{1-x}Al_xO_3$ (x = 0.1). $1-x(CaTiO_3)$-$x(Li_{0.5}La_{0.5})TiO_3$ compositions (x = 0.2–0.8) exhibit ε_r = 245, $Q\times f_o$ = 2750 GHz, and τ_f = 0.75 ppm/°C at x = 0.6 [10]. A niobate-based system, $Ca(Fe_{1/2}Nb_{1/2})O_3$ has ε_r = 40, the $Q\times f_o$ = 20000 GHz, and τ_f = -76 ppm/°C [11]. Similarly, Nb- and Ga-modified $CaTiO_3$ sintered temperature 1350–1475 °C for 4 h possess a good set of MW properties i.e., ε_r = 52, $Q\times f_o$ = 23,595 GHz and τ_f = -4.9 ppm/°C [12].

Another system, $CaTiO_3$-$Ca(Zn_{1/3}Nb_{2/3})O_3$ was investigated for MW dielectric properties which revealed ε_r = 51, $Q\times f_o$ = 10860 GHz and τ_f ~-6 ppm/°C [13]. The effect of niobium doping in $CaTiO_3$ is very prominent at the B-site. Therefore, we have doped Ti^{+4} by $(Al_{1/2}Nb_{1/2})^{4+}$

* Corresponding author. *E-mail address:* akbarkhan712@gmail.com (A. Khan)
Received 9 October 2021; Received in revised form 5 November 2021; Accepted 6 November 2021.

https://doi.org/10.53063/synsint.2021.1467

to maintain charge balance, and its effect on the microwave dielectric properties was investigated.

2. Experimental techniques

$CaTi_{1-x}(Nb_{1/2}Al_{1/2})_xO_3$ (x = 0.1, 0.2, 0.3, 0.4, and 0.5) ceramic solid solution was prepared via solid state sintering route. For accurate weighing, the raw materials $CaCO_3$, TiO_2, Nb_2O_5 and Al_2O_3 were dried to remove the moistures and hydroxide (if any). The dried powders were weighted and then ball-milled in isopropanol for 24 h using Y-toughened zirconia balls as a grinding media. After mixing, the powders were calcined at 950 °C for 6 h in alumina crucible at a heating/cooling rate of 10 °C/min. The calcined powders were re-milled and then pressed into pellets at a pressure of 100 MPa in cylindrical stainless-steel die with a 10 mm in diameter using a uniaxial pellet press. Green pellets were sintered in the temperature range of 1450–1650 °C for 8 h in a muffle furnace to achieve maximum density. The density of the sintered discs was measured using a high precession densitometer (DM 500) using the Archimedes method. For phase identification of the samples, x-ray diffractometer (PANalytical X´pert Pro) was used. The diffraction patterns were recorded at room temperature (RT) using Cu-Kα radiations (λ = 1.5405 Å) in 2θ range from 10–70 °, at a small step size 0.05 ° and scanning time of 3 sec/step. Raman spectra were recorded at RT using a Renishaw Raman microscope with a diode 514 nm excitation Ar laser. The exposure time was 10 s for each sample. Surface morphology was studied using scanning electron microscope JEOL (JSM-6460LV). Before SEM analysis, pellets were polished, thermally etched and carbon coated. MW dielectric properties (ε_r, $Q\times f_o$, and τ_f) of the sintered sample were measured using an Advantest-R3767CH vector network analyzer. τ_f was measured in temperature range from RT to 80 °C.

3. Results and discussion

X-Ray Diffraction (XRD) patterns of the sintered $CaTi_{1-x}(Nb_{1/2}Al_{1/2})_xO_3$ (CTNA) for x = 0.1–0.5 ceramics are shown in Fig. 1. The Braggs reflections matched PDF # 86-1393 for all samples which confirm the orthorhombic structure having space group Pbnm (No. 62). XRD peaks slightly shifted to higher 2θ angles with increase in x, which may be attributed to smaller ionic radius of $[Al_{1/2}Nb_{1/2}]^{4+}$ (r = 0.585 Å) in comparison to Ti^{4+} (r = 0.605 Å) [14]. Thus, the unit cell volume decreased with increase in x.

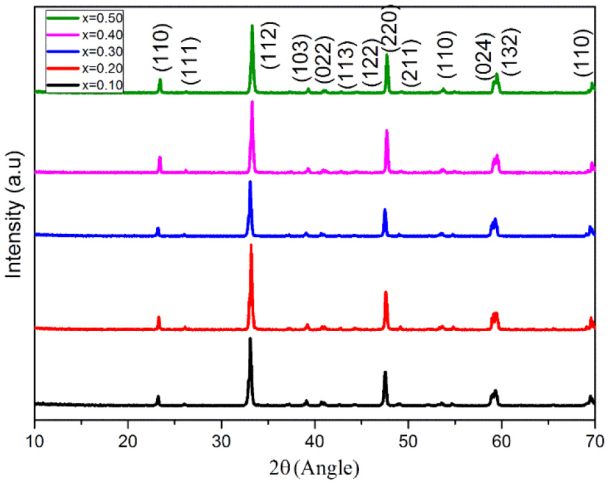

Fig. 1. XRD patterns of CTNA samples, sintered at their optimum sintering temperature.

Raman spectroscopy analysis was also carried out to further confirm the symmetry of the samples, Fig. 2. A total of 13 Raman modes were detected (Table 1) which are in agreement with previous studies [12, 15, 16]. The band near 637 cm^{-1} for the sample with x = 0.1 can be allocated to the Ti–O symmetric stretching mode [17], which disappeared as the $Ti4^+$ is replaced by the dopant Al^{3+} and Nb^{5+}. The intensity of the band near ~804 cm^{-1} increased with increasing concentration which is assigned to the rotation of BO_6 octahedra [12]. As the ionic radius of Al^{3+}, Nb^{5+} and Ti^{+4} is different; therefore, their bands will appear at slightly different frequencies. Due to non-equivalence their vibration may become Raman active modes as stated by Zheng et al. [16]. The band near 838 cm^{-1} starts appearing as x is increased which is due to multiple cations at the B-site, as reported for $CaTiO_3$ based compounds having more than one cations at the Ti-site, known as A1g mode [18]. Raman bands at ~244, 471, and 804 cm^{-1} may be associated with the asymmetric and symmetric breathing of octahedra [19]. The peaks at 499 cm^{-1} may be attributed to Ti–O_3 torsional mode which shifted to 539 cm^{-1} which is due to the fact that Ti–O–Ti bond length is larger than Al–O–Nb [20]. Cockayne et al. [21] suggested that it may also be due to cation ordering of Al–O–Nb bond. The bands at ~121, 149, 178, 224, 277, and 337 cm^{-1} are assigned to O–Ti–O bending and 244 cm^{-1} may be attributed the Ca–TiO_3 lattice mode [12, 16].

SEM micrographs of the thermally etched and polished CTNA samples sintered at 1650 °C for 8 h are shown in Fig. 3. Some voids were observed in the SEM images, thus leading to a low density, consistent with the apparent density of the sample. A granular like connected grains can be seen in the microstructure of sample x = 0.1. For sample x = 0.2 and 0.3, hexagon like grains were formed and the grain size increased. In comparison to sample x = 0.1, the x = 0.2 sample has less voids and hence greater density. With further increase in x, a clear increase in the grain size as well as a slight decrease in density was observed. For sample x = 0.5, well-connected grains with some voids were observed; however, the apparent density was still lower due to these larger voids.

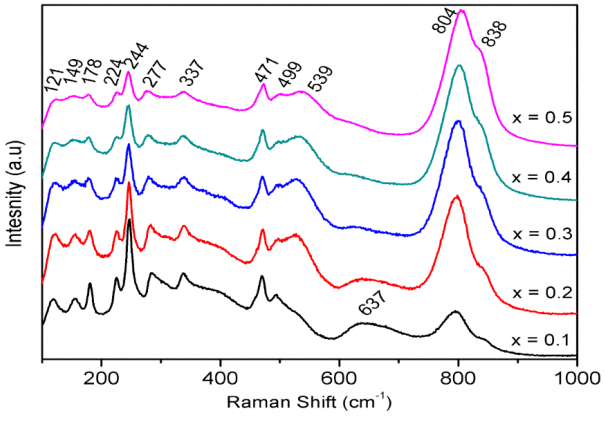

Fig. 2. Raman spectra of CTNA samples.

Table 1. Comparison of the Raman bands of CTNA with literature.

Band	1	2	3	4	5	6	7	8	9	10	11	12	13	Ref.
CTNA	121	149	178	224	244	277	337	471	499	539	637	804	838	Present work
CTNG	123	153	180	225	249	279	345	461	485	543	641	792	817	[12]
YCT-NA	-	163	183	227	247	288	339	470	494	509	641	-	825	[16]

MW dielectric properties of CTNA samples are given in Table. 2. At x = 0.1, the sample possess ε_r = 55 which increased with increase in x from 0.1 to 0.2. The only possible reason for the increase in relative permittivity may be the lower density of x = 0.1 sample in comparison to x = 0.2 which is also evident from the micrograph and observed density of these samples. With further increase in x from 0.2 to 0.5, ε_r gradually decreased. Also, ε_r strongly depends on ionic polarizability and molar cell volume. In the present case, both ionic polarizabilities per unit volume decreased due to the substitution of $(Al_{1/2}Nb_{1/2})^{4+}$ for Ti^{4+} [14]. On the other hand, the $Q \times f_o$ showed similar trend like ε_r for

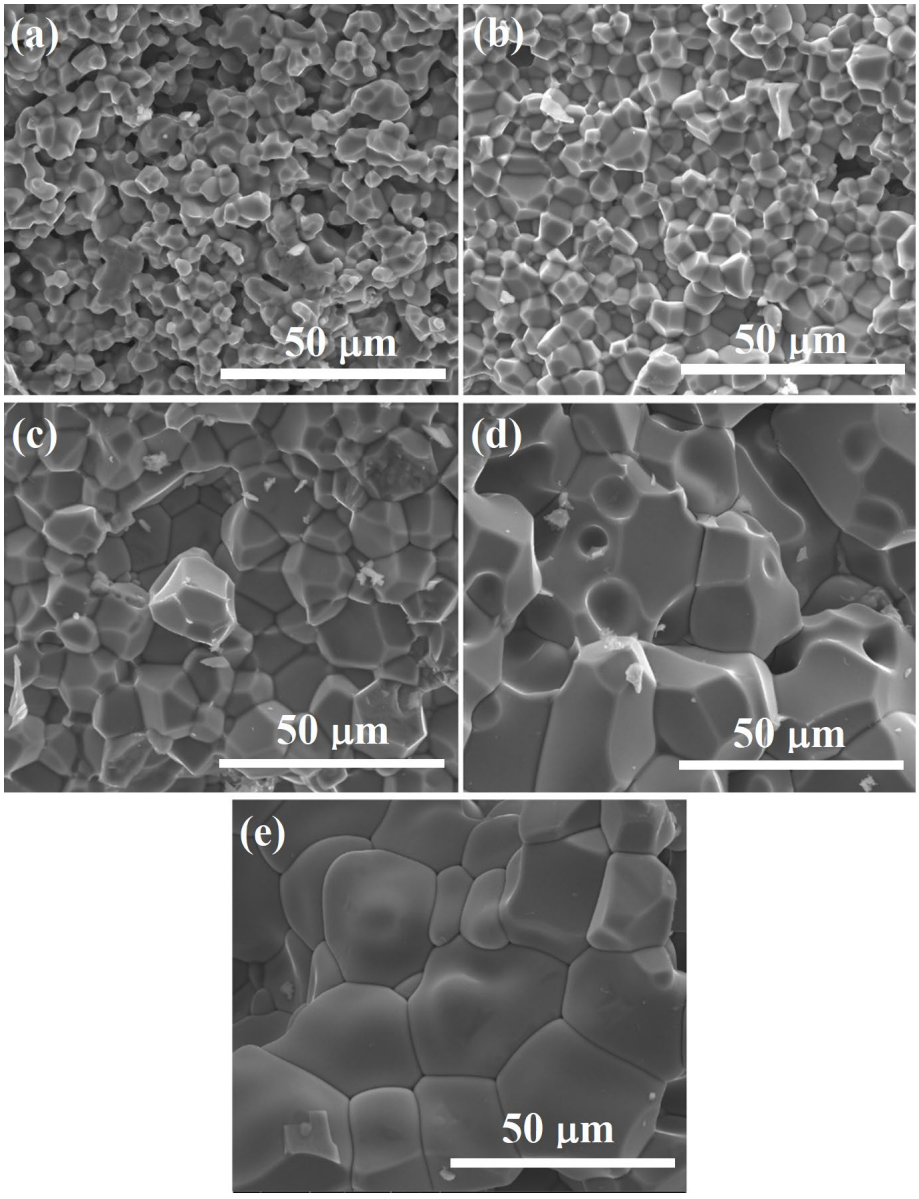

Fig. 3. SEM images of CTNA samples, sintered at 1650 °C for 8 h; x = a) 0.1, b) 0.2, c) 0.3, d) 0.4, and e) 0.5.

Table 2. MW dielectric properties of CTNA.

Sample (x)	Sintering temperature (°C)	Sintering time (h)	Density (g/cm^3)	ε_r	Q×f_o (GHz)	τ_f (ppm/°C)
0.1	1650	8	2.88	55.11	7754	+456.6
0.2	1650	8	3.548	75.08	11487	+274.3
0.3	1650	8	3.498	57.80	11612	+137.13
0.4	1650	8	3.35	45.39	15390	+35.92
0.5	1650	8	2.903	27.09	17378	-2.5

the samples x = 0.1 and 0.2 because Q×f_o is also strongly dependent on density [22]. As the porosity decreased, that quality factor increased. With an increase in x, the quality factor significantly enhanced which may be due to a decrease in lattice harmonic vibrations due to substitution of lower ionic polarizability and smaller ionic radii of Al^{3+} in comparison to Ti^{4+} [23]. Similarly, grain boundaries per unit volume decrease, which limit the conduction and hence improves the quality factor [6]. Generally, ε_r and τ_f have a linear relationship because τ_f is also influenced by the temperature coefficient of relative permittivity [24, 25]. τ_f value decreased from +456.6 to -2.5 ppm/°C which may be attributed to a decrease in tilting angle of BO_6 octahedra [26]. The tolerance factor of CTNA is 0.972 which is higher than CT (0.965); therefore, an anti-phase tilting scheme is expected [27]. Mostly, in this tiling scheme, perovskites exhibit a near zero temperature coefficient of dielectric constant and hence temperature coefficient of the resonance frequency.

4. Conclusions

In the present work, $CaTi_{1-x}(Nb_{1/2}Al_{1/2})_xO_3$ (x = 0.1 to 0.5) were prepared via solid state sintering route. XRD results and Raman results confirmed the formation of single-phase orthorhombic crystal structures (Pbnm). The effect of sintering temperature on the microwave dielectric properties was also investigated. The samples were found to become harder in density; therefore, sintering time was increased. SEM results showed some voids in the microstructures which were associated with the lower density of the samples. ε_r, τ_f decreased and Q×f_o was observed to increase as x from x = 0.2 to x = 0.5. The optimum set of MW dielectric properties was observed for sample x = 0.5 i.e., ε_r ~27, Q×f_o ~17378 GHz and high τ_f ~-2.5 ppm/°C when sintered temperature 1650 °C for 8 h which may be suitable for use in practical applications.

CRediT authorship contribution statement

Akbar Khan: Methodology, Writing – original draft.
Asif Ali: Supervision, Writing – review & editing.
Izaz Khan: Investigation, Writing – review & editing.

Data availability

The data underlying this article will be shared on reasonable request to the corresponding author.

Declaration of competing interest

The authors declare no competing interests.

Funding and acknowledgment

The authors would like to thank the Laboratory of Functional Materials and Devices, Department of Physics, Abdul Wali Khan University Mardan, for their support in this research.

References

[1] F. Kamutzki, S. Schneider, J. Barowski, A. Gurlo, D.A.H. Hanaor, Silicate dielectric ceramics for millimetre wave applications, J. Eur. Ceram. Soc. 41 (2021) 3879–3894. https://doi.org/10.1016/j.jeurceramsoc.2021.02.048.
[2] M.T. Sebastian, R. Ubic, H. Jantunen, Microwave materials and applications, John Wiley & Sons. (2017).
[3] M.T. Sebastian, H. Wang, H. Jantunen, Low temperature co-fired ceramics with ultra-low sintering temperature: a review, Curr. Opin. Solid State Mater. Sci. 20 (2016) 151–170. https://doi.org/10.1016/j.cossms.2016.02.004.
[4] R. Muhammad, Y. Iqbal, Phase, microstructure and microwave dielectric properties of $Ca_{1-x}La_xTi_{1-x/4}O_3$ (x= 0–1) ceramics, J. Mater. Sci: Mater. Elec. 26 (2015) 4870–4874. https://doi.org/10.1007/s10854-015-2995-2.
[5] T. Liu, X.Z. Zhao, W. Chen, A/B site modified $CaTiO_3$ dielectric ceramics for microwave application, J. Am. Ceram. Soc. 89 (2006) 1153–1155. https://doi.org/10.1111/j.1551-2916.2005.00894.x.
[6] R. Muhammad, Y. Iqbal, Microwave dielectric properties of Ga3+ and Ta5+ co-doped $CaTiO_3$, J. Mater. Sci. 51 (2016) 2958–2963. https://doi.org/10.1007/s10853-015-9604-x.
[7] C.-L. Huang, J.-T. Tsai, Y.-B. Chen, Dielectric properties of (1-y)$Ca_{1-x}La_{2x/3}TiO_3$-y$(Li,Nd)_{1/2}TiO_3$ ceramic system at microwave frequency, Mater. Res. Bull. 36 (2001) 547–556. https://doi.org/10.1016/S0025-5408(01)00528-1.
[8] R. Muhammad, Y. Iqbal, Structure and microwave dielectric properties of $Ca_{0.66}La_{0.387}Ti_{0.88}O_3$ ceramics, J. Mater. Sci. Mater. Elec. 26 (2015) 9092–9096. https://doi.org/10.1007/s10854-015-3596-9.
[9] A. Feteira, D.C. Sinclair, M.T. Lanagan, Structure and Microwave Dielectric Properties of $Ca_{1-x}Y_xTi_{1-x}Al_xO_3$ (CYTA) Ceramics, J. Mater. Res. 20 (2005) 2391–2399. https://doi.org/10.1557/jmr.2005.0289.
[10] J. Li, Y. Han, T. Qiu, C. Jin, Effect of bond valence on microwave dielectric properties of (1−x)CaTiO3–x(Li0.5La0.5)TiO3 ceramics, Mater. Res. Bull. 47 (2012) 2375–2379. https://doi.org/10.1016/j.materresbull.2012.05.024.
[11] H. Kagata, J. Kato, Dielectric properties of Ca-based complex perovskite at microwave frequencies, Jpn. J. Appl. Phys. 33 (1994) 5463. https://doi.org/10.1143/JJAP.33.5463.
[12] R. Muhammad, Y. Iqbal, Microwave dielectric properties of $CaTi_{1-x}(Nb_{0.5}Ga_{0.5})_xO_3$ ceramics, Mater. Lett. 153 (2015) 121–123. https://doi.org/10.1016/j.matlet.2015.04.021.

[13] H. Liu, H. Yu, Z. Tian, Z. Meng, Z. Wu, S. Ouyang, Dielectric properties of (1−x)$CaTiO_3$–x$Ca(Zn_{1/3}Nb_{2/3})O_3$ ceramic system at microwave frequency, J. Am. Ceram. Soc. 88 (2005) 453–455. https://doi.org/10.1111/j.1551-2916.2005.00064.x.

[14] R.T. Shannon, C.T. Prewitt, Effective ionic radii in oxides and fluorides, Acta Crystallogr. B. 25 (1969) 925–946. https://doi.org/10.1107/S0567740869003220.

[15] I. Levin, J.Y. Chan, J.E. Maslar, T.A. Vanderah, S. Bell, Phase transitions and microwave dielectric properties in the perovskite-like $Ca(Al_{0.5}Nb_{0.5})O_3$–$CaTiO_3$ system, J. Appl. Phys. 90 (2001) 904–914. https://doi.org/10.1063/1.1373705.

[16] H. Zheng, H. Bagshaw, G. Csete de Györgyfalva, I. Reaney, R. Ubic, J. Yarwood, Raman spectroscopy and microwave properties of $CaTiO_3$-based ceramics, J. Appl. Phys. 94 (2003) 2948–2956. https://doi.org/10.1063/1.1598271.

[17] M. Saleem, Y. Iqbal, S. Qin, X. Wu, R. Muhammad, F. Zhu, Structural phase transition and microwave dielectric properties of $Ca_{1-x}Sr_xTiO_3$ (x=0.1–0.9) ceramics, J. Mater. Sci. Mater. Elec. 26 (2015) 1507–1511. https://doi.org/10.1007/s10854-014-2568-9.

[18] H. Zheng, I. Reaney, G.C. de Györgyfalva, R. Ubic, J. Yarwood, et al., Raman spectroscopy of $CaTiO_3$-based perovskite solid solutions, J. Mater. Res. 19 (2004) 488–495. https://doi.org/10.1557/jmr.2004.19.2.488.

[19] H. Zheng, G.D.C. Csete de Györgyfalva, R. Quimby, H. Bagshaw, R. Ubic, et al., Raman spectroscopy of B-site order–disorder in CaTiO3-based microwave ceramics, J. Eur. Ceram. Soc. 23 (2003) 2653–2659. https://doi.org/10.1016/S0955-2219(03)00149-3.

[20] T. Hirata, K. Ishioka, M. Kitajima, Vibrational spectroscopy and X-ray diffraction of perovskite compounds $Sr_{1-x}M_xTiO_3$ (M=Ca, Mg; 0≤ x≤ 1), J. Solid State Chem. 124 (1996) 353–359. https://doi.org/10.1006/jssc.1996.0249.

[21] S. Prosandeev, E. Cockayne, B.P. Burton, S. Kamba, J. Petzelt, et al., Lattice dynamics in $PbMg_{1/3}Nb_{2/3}O_3$, Phys. Rev. B. 70 (2004) 134110. https://doi.org/10.1103/PhysRevB.70.134110.

[22] R. Muhammad, Y. Iqbal, Preparation and characterization of K-substituted $NaCa_4Nb_5O_{17}$ microwave dielectric ceramics, J. Mater. Sci. Mater. Elec. 24 (2013) 2322–2326. https://doi.org/10.1007/s10854-013-1096-3.

[23] R.D. Shannon, Dielectric polarizabilities of ions in oxides and fluorides, J. Appl. Phys. 73 (1993) 348–366. https://doi.org/10.1063/1.353856.

[24] E. Colla, I. Reaney, N. Setter, Effect of structural changes in complex perovskites on the temperature coefficient of the relative permittivity, J. Appl. Phys. 74 (1993) 3414–3425. https://doi.org/10.1063/1.354569.

[25] R. Muhammad, Y. Iqbal, I.M. Reaney, New low loss $A_9B_9O_{31}$ (A=La; B=Ti, Mg, Sc, Fe, Al, Ga) ceramics for microwave applications, J. Alloys. Compd. 646 (2015) 368–371. https://doi.org/10.1016/j.jallcom.2015.06.038.

[26] I.M. Reaney, E.L. Colla, N. Setter, Dielectric and structural characteristics of Ba-and Sr-based complex perovskites as a function of tolerance factor, Jpn. J. Appl. Phys. 33 (1994) 3984. https://doi.org/10.1143/JJAP.33.3984.

[27] I.M. Reaney, D. Iddles, Microwave dielectric ceramics for resonators and filters in mobile phone networks, J. Am. Ceram. Soc. 89 (2006) 2063–2072. https://doi.org/10.1111/j.1551-2916.2006.01025.x.